Received: 11 July 2022 | Revised: 3 May 2023 | Accepted: 18 May 2023

DOI: 10.1111/geb.13711

Global Ecology and Biogeography | A Journal of Macroecology | WILEY

RESEARCH ARTICLE

Earthquake disturbance shifts metabolic energy use and partitioning in a monodominant forest

Meng Xu[1] | Robert B. Allen[2] | Erica A. Newman[3]

[1]Department of Mathematics, Pace University, New York, New York, USA

[2]Independent Researcher, Lincoln, New Zealand

[3]Department of Integrative Biology, University of Texas at Austin, Austin, Texas, USA

Correspondence
Meng Xu, Department of Mathematics, Pace University, 41 Park Row, New York, NY 10038, USA.
Email: mxu@pace.edu

Handling Editor: Angelica Gonzalez

Abstract

Aim: Both macroecology and disturbance ecology have long been used to characterize population- and community-level patterns across scales, but the integration of both approaches in characterizing disturbed ecosystems is rare. Here, we use the maximum entropy theory of ecology (METE) to model the individual size distribution (ISD) of trees in pre- and post-disturbance tree populations and estimate the corresponding metabolic scaling exponents.

Location: New Zealand.

Time Period: 1987–1999.

Major Taxa Studied: Mountain beech (*Fuscospora cliffortioides* Nothofagaceae).

Methods: METE uses information entropy and empirical macro-state variables to constrain predictions of ecological distributions related to biodiversity. METE has successfully predicted a range of biodiversity metrics in static or relatively undisturbed conditions. However, METE can fail to accurately model ecological patterns in disturbed ecosystems. We extend existing theoretical predictions to a highly disturbed ecosystem by treating the metabolic scaling exponent and Lagrange multipliers as free parameters in METE.

Results: We showed that the fully parameterized METE (FP-METE) model reasonably predicted the ISD of mountain beech populations in a monodominant forest after a strong earthquake, which restructured the forest. Furthermore, the FP-METE model revealed that decreasing metabolic scaling exponent drove the substantial decline of total metabolic rate energy and the redistribution of energy towards smaller trees after the earthquake. Increased number of small trees was not sufficient to capture the full impact of disturbance on forest energy use.

Main Conclusions: Our FP-METE model applies an informatics approach to estimate the metabolic scaling relationship. We find that instead of maintaining a fixed value, the metabolic scaling exponent is variable among populations, and declines significantly after an earthquake disturbance. This leads to major shifts in the total population metabolic energy and energy distribution. With this approach, we now have the opportunity to advance beyond categorizing forms of mathematical distributions that describe biodiversity patterns and move into a predictive framework where the true constraints on ecosystems and their dynamics emerge.

KEYWORDS
constraint-based model, earthquake disturbance, ecological informatics, individual size distribution, Lagrange multipliers, maximum entropy, metabolic rate energy, mountain beech, New Zealand

1 | INTRODUCTION

Ecological disturbances, whether caused by natural phenomena or human activities, bring about marked changes in the structure and functioning of ecosystems. Examples include changes in mortality (Courtois et al., 2007; Stillman et al., 2007), resource availability (Wilson & Tilman, 1991, 1993; Wright et al., 2015), biodiversity (Barlow et al., 2016; Cardinale & Palmer, 2002; Dornelas, 2010; Thom & Seidl, 2016), habitat (Brawn et al., 2001; Yamamoto, 2000), and the functioning of communities and ecosystems (Alberti, 2005; Fitzhugh et al., 2001; Helmus et al., 2010; Seidl et al., 2014; Tait & Schiel, 2011; Villnäs et al., 2013; Winfree et al., 2007). The Anthropocene is characterized by increasing human-induced alterations of the Earth System (Hamilton, 2015; Steffen et al., 2007), so understanding the roles of natural disturbance and anthropogenic changes in ecosystems has become increasingly important for the design of conservation and management policies from local to global scales (Attiwill, 1994; Danneyrolles et al., 2019; Newman, 2019; Resh et al., 1988; Turner, 2010).

Tests of macroecological predictions provide a unique prism for examining the impacts of disturbance, since functional changes imposed by disturbance may lead to variation of ecological patterns and the mathematical forms that describe them (Hubbell et al., 1999; Jenkins, 2011; Rybicki & Hanski, 2013; Santini et al., 2017; Supp & Ernest, 2014). Research that integrates macroecological approaches and ecological patterns to disturbance ecology has been limited by three factors. First, a major goal of macroecological studies is to extract consistent patterns in biodiversity metrics across multiple taxa or biological communities, often from many disparate datasets, and to examine how such metrics vary across spatial and temporal scales. Such meta-analyses often target undisturbed ecosystems, or represent ecosystems with unreported, unknown or mixed disturbance history, making it difficult to detect or analyse any macroecological signals exerted by a specific disturbance. Second, the effects of disturbances on ecosystems are often long-lasting 'legacy' effects (e.g. Cuddington, 2011; Johnstone et al., 2016) and may exhibit time delays (Zeng et al., 2017). For example, decadal data are often necessary to document the effect of disturbance events on forest ecosystems (Kleinman et al., 2019). Third, on the modelling front, existing ecological theories that aim to explain macroecological patterns (those that relate species richness and abundance to area or metabolic energy use, for example) mostly assume that the studied communities or species are in equilibrium (e.g. demographic equilibrium theory; see Coomes et al., 2003; Muller-Landau et al., 2006). Models that incorporate disturbance into theoretical constructs are less often explored (but see DeAngelis et al., 1985).

The maximum entropy theory of ecology (METE) is a constraint-based theory (Harte, 2011; Harte et al., 2008; Harte & Newman, 2014) and is considered one of the unified theories in ecology (McGill, 2010). The idea underlying METE follows from the logic of thermodynamics, in which relationships among macroscopic 'state variables' are derived from distributions of microstates, with probability distributions obtained by maximization of information entropy (Jaynes, 1957; Shannon, 1948) using the Lagrange multiplier method (Bertsekas, 2014). In ecological contexts, METE is used to search for the least-biased core distribution functions subject to the constraints of macro-state ecological variables of the studied community. These macro-state variables include the total area (A_0) of a defined region, the number of species (S_0), the total number of individuals (N_0) and the total metabolic rate energy (E_0) in that region (consequently the theory is dubbed as the ASNE version of METE, see Brummer & Newman, 2019; Harte, 2011). The core functions of METE can be summarized to predict various macroecological patterns, such as the species–area relationship (Harte et al., 2009; Harte & Kitzes, 2015; Wilber et al., 2015), the species–abundance distribution (White et al., 2012; Xiao et al., 2015), the species-level spatial abundance distribution (McGlinn et al., 2013, 2015), the individual metabolic rate distribution (Harte et al., 2017; Newman et al., 2014) and the individual size distribution (ISD; Xiao et al., 2015). Recent studies show that METE fails to give accurate predictions in disturbed ecosystems (Brush et al., 2022; Franzman et al., 2021; Newman et al., 2020).

METE is a useful tool for modelling energy flux in ecological systems, because it contains the metabolic rate of an individual organism as one of the micro-state variables in the formulation. Energy flux (or E_0 in METE) is quantified by summing the metabolic rate of all individuals in a community or population. In food webs, energy flux is useful for studying biodiversity and ecosystem functioning (Barnes et al., 2018). In forest ecosystems, the total metabolic rate is crucial to understanding the carbon cycle and its impact on climate change. Other plant measurements, such as basal area or biomass, do not adequately measure the rate of resource use because they are based mainly on the growth rate that captures net energy assimilation rather than energy dissimilation (Deng et al., 2008). To test its energetic predictions, METE transforms the predicted individual metabolic rates to predicted individual body sizes using a metabolic scaling relationship (metabolic rate as a power function of body size) and compares the predicted distribution of individuals' sizes to the observed ISD. The metabolic scaling exponent is assumed to be a universal constant suggested by the metabolic scaling theory (MST; West et al., 1997, 1999). However, the universality of the metabolic scaling exponent has been refuted by overwhelming empirical evidence (Bokma, 2004; Glazier, 2005, 2022; White,

Cassey, et al., 2007). This assumption casts doubt on the usefulness and generality of METE's metabolic energy rate prediction. As Harte et al. (2017) stated, '*We do not know how much of the discrepancy* (between the predicted and observed ISD) *is attributable simply to inaccuracies in the tree allometry and metabolic scaling rule that were used to replace metabolic rate with basal area.*'

In this work, we study the usefulness of the ASNE version of METE (Harte, 2011) in modelling macroecological patterns and predicting the metabolic energy use patterns of a disturbed forest, using the mountain beech tree size data of a monodominant forest before and after (with a 12-year gap) a strong earthquake (called pre- and post-earthquake data, respectively) in New Zealand. Specifically, we apply the partially parameterized METE (PP-METE) model, in which the metabolic scaling exponent is a free parameter (first developed by Xu, 2020), and introduce the new fully parameterized METE (FP-METE) model, in which both the metabolic scaling exponent and the Lagrange multipliers are free parameters. In the original formulation of METE, the Lagrange multipliers represent the coefficients of the constraint equations and are solved numerically (Harte, 2011). Instead of assuming a constant metabolic scaling exponent, as in the testing of the original METE, we estimate the exponent from the PP-METE and FP-METE models by fitting the corresponding model predictions to the observed ISD. Xu (2020) showed that the PP-METE models described the ISD of trees within communities in two separate forests reasonably accurately; and Xu et al. (2021) used the PP-METE models to successfully predict the form and parameters of the scaling relationship between the mean and the variance of the individual metabolic rate across tree communities in a tropical forest.

The success of parameterized METE models in predicting the observed pattern would indicate that their estimates of metabolic scaling exponent are empirically plausible. This, in turn, would shed new light on the pattern of resource use within the community or population. In particular, the concept of 'energy equivalence' posits that energy use for a population is invariant with respect to body size (White, Ernest, et al., 2007), a hypothesis that follows from combining the Damuth's Rule (Damuth, 1981) and the Klieber's Law (Kleiber, 1947), describing the abundance–size relationship and the metabolic scaling relationship, respectively. The problems with this approach are as follows: (1) The metabolic scaling relationship is often assumed from existing theory (e.g. MST) rather than tested against empirical data and (2) the combination of the two relationships falls into the fallacy of averages, since the two relationships may be analysed at different scales or have scatter around true power-law relationships (Medel et al., 1995). Indeed, energy equivalence has found equivocal empirical results in various taxa and environments (Deng et al., 2008; Ehnes et al., 2014; Ernest et al., 2009; Ghedini et al., 2020; Hayward et al., 2009; Russo et al., 2003; Sewall et al., 2013). In addition, the concept and methodology of energy equivalence have been debated (Isaac et al., 2013; Sewall et al., 2013).

With the estimated metabolic scaling exponent from our model, we can overcome the above issues by calculating the total metabolic rate as the sum of the individual metabolic rates (which is proportional to the individual body size raised to the metabolic scaling exponent) from individuals within a specific group. This allows us to directly assess the validity of energy equivalence and the metabolic energy distribution at different states of the studied ecosystem.

The specific objectives of this work are as follows: (1) To evaluate the performance of the parameterized METE models in describing the ISD for undisturbed (pre-earthquake) and disturbed (post-earthquake) mountain beech populations and (2) to detect any changes in the energy use and partitioning among forest plots before and after the earthquake by using the metabolic scaling exponent estimated from the FP-METE model. We find that the FP-METE model predicts the observed distributions with reasonably high accuracy, and that the predicted change in the metabolic scaling exponent leads to a substantial decrease in total metabolic rate energy use and the restructuring of how energy is partitioned among individuals after the disturbance. Our FP-METE model provides a novel method of using individual-level size data to infer metabolic scaling and energy use of tree populations, therefore enhancing the predictive scope of METE.

2 | METHODS

2.1 | Data

Individual tree data were collected from Craigieburn Forest Park, which contains a monodominant mountain beech (*Fuscospora cliffortioides* Nothofagaceae; syn. *Nothofagus solandri* var. *cliffortioides*) forest canopy, in the eastern part of the South Island, New Zealand. Tree sampling was carried out in 250 plots (each 20 m by 20 m) located throughout the forest. Our representative sample of many trees on many plots over 9000 ha of the forest allowed us to incorporate the variable nature of forest dynamics (Allen et al., 2020). During the austral summers starting 1974, within each plot, each tree (stem) with a diameter at breast height of at least 3 cm was measured for diameter at breast height and identified to species. Allen et al. (2020) provided detailed information on the forest, the sampling method and data accessibility.

The Arthur's Pass earthquake was a strong earthquake (M_w 6.7) that occurred on 18 June 1994 in the Southern Alps region of New Zealand (Arnadottir et al., 1995), with its epicentre near the northwestern corner of the sampled area. Hurst et al. (2011) showed that pre-1987 was a relatively stable period in the forest, whereas 1994–1999 was a period with a marked decline in mean plot-level basal area and stem biomass related to the earthquake. During the earthquake, 24% of all trees were killed and 23% of trees were injured near the epicentre. This damage was concentrated, with 11% of the plots having >80% live stem biomass mortality (Allen et al., 1999). To analyse the impact of the earthquake on the forest size structure, we used tree size data from the 250 plots measured in 1987 and remeasured in 1999, and called them respectively the pre-earthquake data and post-earthquake data. Pre-earthquake data (from all 250 plots)

included seven species and 15,575 trees, of which 15,512 trees (99.60%) were mountain beech. Post-earthquake data (from all 250 plots, including three plots with no trees due to landslides caused by the earthquake) included 10 species and 16,877 trees, of which 16,789 trees (99.48%) were mountain beech. The increase in tree abundance can be attributed to a recruitment cohort following pre-1980 disturbance events (Allen et al., 2020).

To study the size distribution of individual trees for pre- and post-earthquake data, we used three different size metrics. In addition to the diameter at breast height (in centimetres), we also calculated the height (in meters) and aboveground biomass (in kg C) of each tree from its diameter at breast height using equations 12 and 11, respectively in Coomes et al. (2012; developed by Harcombe et al., 1997). In the pre- and post-earthquake data separately, we defined all trees (regardless of species) as a community and all mountain beech trees as a population. We focus on population-level analysis throughout the paper.

2.2 | Overview of the METE and MST

An ecosystem structure function defines the metabolic predictions of METE as the joint distribution of a species having n individuals and an individual (from a species with n individuals) having a certain metabolic rate ε (Brummer & Newman, 2019). METE then solves the ecosystem structure function by maximizing its Shannon information entropy (Jaynes, 1957, 2003) subject to the mean species abundance and mean species metabolic rate energy within a community. This joint distribution can then be used to derive other distributions and scaling patterns that characterize a community or population, such as the species abundance distribution, individual metabolic rate distribution and ISD.

Theoretical predictions of METE have been extensively compared against empirical data (see Introduction). In terms of the metabolic predictions, Xiao et al. (2015) tested several predictions of METE and evaluated the goodness of fit of community- and population-level ISD (called intraspecific ISD therein) separately using multiple data sets. They found that the performance of METE was equivocal: The predicted ISD resembled the observed ISD at the community level, but not at the population level. Newman et al. (2014) showed that the individual metabolic rate distribution predicted by METE behaved differently at the community level (containing multiple species) and the population level (considering each species individually).

METE characterizes individual organisms through their metabolic rates and predicts the individual metabolic rate distribution. However, individual metabolic rates are difficult to measure from field data (Cottingham & Zens, 2004). Additionally, metabolic rate data are often recorded at the species level, neglecting the variation of metabolic rate between conspecifics or habitats. These issues make it challenging to evaluate the metabolic rate predictions of METE against empirical data. To examine the usefulness of METE in predicting individual-level patterns, the predicted metabolic rate distribution needs to be transformed to a normalized size distribution (i.e. ISD), using the metabolic scaling relationship between metabolic rate and body size. The original METE (Harte, 2011) achieves this transformation using the scaling exponent from the MST (West et al., 1997, 1999).

MST predicts that the individual metabolic rate scales as a power function with individual body mass, with a universal exponent of 0.75. Predictions of MST are derived from a branching network model that is applicable to both mammals and vascular plants. In plant systems, for example, using the allometric scaling relationships between the plant's geometric dimensions (e.g. branch radius, plant mass, and tree height; see table 1 in West et al., 1999), MST predicts that the metabolic rate scales proportionally with the plant diameter raised to the exponent of 2, with the plant height raised to the exponent of 3, and with the plant aboveground biomass raised to the exponent of 0.75. For metabolic rate-biomass scaling, Harte et al. (2022) showed that the exponent of 0.75 performs better for certain METE predictions than does an alternative exponent of 0.67.

Testing of METE has been performed by inserting the universal metabolic scaling exponents from MST into the predicted ISD, which can then be compared to the observed ISD to evaluate the goodness of fit of the prediction. Such treatment, although mathematically convenient, poses difficulty in assessing the usefulness of the METE's predictions of ISD, since it would be impossible to determine whether the discrepancy between the observed and predicted ISDs is due to the METE's formulation, or the mismatch between the hypothesized metabolic scaling exponent and the empirical data (Harte et al., 2017).

2.3 | Parameterized METE: Models and evaluation

Xu (2020) adopted the power-function form of the metabolic scaling relationship and incorporated the metabolic scaling exponent (b) as a free parameter in the METE framework to accommodate any mismatch between data and MST. Here, we extended Xu's models by treating both b and the two Lagrange multipliers (λ_1 and λ_2) that arise from solving the ecosystem structure function in METE (see Table 1) as free parameters. To distinguish them, we call the model by Xu (2020) 'partially parameterized METE' (PP-METE) model and the new extended model 'fully parameterized METE' (FP-METE) model. In this work, we evaluate the performance of the original METE and the parameterized METE (i.e. PP-METE and FP-METE) in modelling mountain beech ISD, and we use the FP-METE model to detect changes of metabolic scaling and energy use in the pre- and post-earthquake mountain beech populations. There are two crucial differences between the three maximum entropy models: (1) During model testing, the original METE assumes that b is a universal constant from the MST (see previous section on MST); while PP-METE and FP-METE obtain the maximum likelihood estimate of b by fitting the corresponding predicted ISD to the observed ISD. (2) The original METE and the PP-METE estimate λ_1 and λ_2 using the mean constraints on species abundance and species metabolic rate at the community level (see equations 7.2–7.3 and equations 7.16–7.17

TABLE 1 Notations used in this paper. Definition shows the name of each notation, and description/formula gives its meaning. In the PP-METE and FP-METE models, *b* is treated as a free parameter. In the original METE model, *b* takes constant values predicted from the MST, with a value of 2, 3, or 0.75 when the size is measured by diameter at breast height (dbh), height (ht), or aboveground biomass (agb), respectively.

Category	Notation	Definition	Description/formula
Observed variable	*size*	Individual size	Size of individual tree
	s	Rescaled individual size	*Size*/min(*size*), where min(*size*) is the minimum individual size of mountain beech
	dbh	Individual diameter at breast height	Diameter of individual tree measured at breast height (in cm)
	d	Rescaled individual diameter at breast height	See formula of *s*
	n	Species abundance	Number of individuals of mountain beech
	T	Temperature	Mean annual temperature in Kelvin (K)
	alt	Altitude	Above sea altitude, here used as synonym for elevation (in m)
Model parameter of METE	*b*	Metabolic scaling exponent	Exponent in the scaling relationship of metabolic rate as a power function of size (free parameter in PP-METE and FP-METE)
	λ_1	First Lagrange multiplier	Coefficient for the constraint of mean species abundance (used in METE and PP-METE at the community level)
	λ_2	Second Lagrange multiplier	Coefficient for the constraint of mean metabolic rate per species (used in METE and PP-METE at the community level, and in FP-METE at the population level)
Estimated variable	*ht*	Individual tree height	Tree height (in m) calculated as $1.35+16.66(1-0.00076\times(alt-640))\,(1-\exp(-0.059 dbh^{1.21}))$ (equation 12 in Coomes et al., 2012)
	h	Rescaled individual height	See formula of *s*
	agb	Individual tree aboveground biomass	Aboveground biomass (in kg C) calculated as $0.0179\,(dbh-0.231)^{1.9204} ht^{0.9602}+0.416$ (equation 11 in Coomes et al., 2012)
	m	Rescaled individual aboveground biomass	See formula of *s*
	ε	Rescaled individual metabolic rate	s^b
	E_0	Total rescaled metabolic rate energy	Σs^b, where summation is over individuals within a plot or from all plots
	B	Total temperature-adjusted metabolic rate energy	$\Sigma(size)^b e^{-E/kT}$, where *E* is the activation energy (≈0.32 eV) and *k* is the Boltzmann's constant (8.6×10^{-5} eVK^{-1}). Summation is over mountain beech trees
	c	Slope of energy–size relationship	Slope of the linear relationship of $\log(E_0)$ against $\log(s)$

Abbreviations: FP-METE, fully parameterized maximum entropy theory of ecology; MST, metabolic scaling theory; PP-METE, partially parameterized maximum entropy theory of ecology.

in Harte, 2011), then feed the estimated λ_2 into their respective population-level ISD predictions, while the FP-METE obtains the maximum likelihood estimates of λ_2 and *b* directly by fitting the corresponding prediction to the observed ISD at the population level. In other words, in the original METE and PP-METE, the predicted mountain beech ISD is based on community-level estimates of λ_1 and λ_2. In FP-METE, the predicted mountain beech ISD does not depend on community-level parameters, and hence is self-contained.

METE predicts the mountain beech ISD as follows:

$$\rho(s) = bs^{b-1} n\lambda_2 \frac{e^{-\lambda_2 n s^b}}{e^{-\lambda_2 n} - e^{-\lambda_2 n}\sum s^b}. \quad (1)$$

Here, Equation 1 is METE's exact prediction of the population-level ISD (see the derivations in the supporting information of Xu, 2020) and *s* is the rescaled individual size (see all notations in Table 1). We

emphasize that the original METE, PP-METE and FP-METE use the same formula (Equation 1) but differ in their treatments of b and the Lagrange multipliers, resulting in zero, one and two free parameters in the respective model. In addition, the form of Equation 1 is similar to the probability density function of the Weibull distribution (Forbes et al., 2011). For a more detailed mathematical comparison of the three METE models, see Appendix S1 in the Supporting Information (SI).

The model fitting procedure is as follows: for mountain beech in the pre- or post-earthquake data separately, using each size measure (d, h, or m), we fitted the PP-METE model and the FP-METE model (Equation 1) to the individual size data and obtained the maximum likelihood estimate of b (one from each model). For PP-METE, we first obtained the community-level estimates of λ_1 and λ_2 and substituted λ_2 into Equation 1, before estimating the population-level b. To assess the effect of sampling variation on the model fitting (and to calculate the interval estimate of b), we created 1000 bootstrap samples of the individual size data from the pre- and post-earthquake community separately. Each bootstrap sample contained the size data of 250 plots that were randomly selected with replacement from the actual 250 plots of the study area. We refitted each parameterized METE model (PP-METE and FP-METE) to the corresponding mountain beech size data from each bootstrap sample.

We evaluated the performance of the parameterized METE models (PP-METE and FP-METE) in three ways. First, we fitted the original METE model (b being a fixed constant in Equation 1) and four phenomenological models (exponential, power-law, Weibull and quasi-Weibull) separately to the mountain beech size data, before and after the earthquake. We analysed these four purely statistical distribution models because they have been used to describe size distributions in empirical data (Bailey & Dell, 1973; Enquist & Niklas, 2001; Lai et al., 2013; Moser Jr, 1972; Muller-Landau et al., 2006), as well as to reveal demographic processes or disturbance effect on the size distribution (Coomes et al., 2003; Kohyama et al., 2003; Muller-Landau et al., 2006). For example, it was hypothesized that the power-law distribution reflects asymmetric competition and that the exponential distribution is a consequence of external disturbance (Coomes et al., 2003). All models were left-truncated and fitted to the observed rescaled ISD with a lower bound at one. For example, tree diameter is rescaled as (diameter at breast height)/min(diameter at breast height). For diameter at breast height and aboveground biomass, the minimal value was identical between pre- and post-earthquake populations. For height, the minimal value differed slightly between pre- and post-earthquake populations. We compared the parameterized METE models with other models using the Akaike information criterion corrected for sample size (AICc) and AICc weight (which represents the relative likelihood of a model). The model with the lowest AICc (and highest AICc weight) is deemed the best-performing model. To evaluate the effect of sampling, each model was refitted to each of the 1000 bootstrap samples and the percentage of its relative rank was recorded.

Second, we calculated the quantiles of each parameterized METE model and compared them with the observed sizes using the coefficient of determination: $R^2 = 1 - \frac{\sum_i[(\text{observed}_i)-(\text{quantile}_i)]^2}{\sum_i[(\text{observed}_i)-\overline{\text{observed}_i}]^2}$, where observed_i is the ith observed rescaled size and quantile_i is the ith quantile from the model prediction. The summation is taken over all mountain beech trees. A high R^2 value would indicate that predicted individual sizes by the PP-METE model or the FP-METE model are close to the observed values. A low R^2 value would indicate that predicted individual sizes of the PP-METE model or the FP-METE model deviate from the observed values. A negative R^2 means that the prediction is worse than the mean of the observations. For comparison, we also calculated R^2 using quantiles from the original METE models and the four other phenomenological models.

Third, we calculated the cumulative distribution function from each parameterized METE model and compared the function with the observed rescaled size data using the one-sample Kolmogorov–Smirnov (K–S) test. The one-sample K–S test is used to test whether or not a sample has likely been drawn from a given distribution. When the p-value of a K–S test is greater than 0.01, we do not reject the hypothesis that the size data follow the same distribution as the prediction from the parameterized METE models. Otherwise, the p-value suggests that the model prediction is a poor approximation of the observation. Since ties are present in the size data, p-values are approximate and not exact. Hence, we also calculated the K–S test statistic, which represents the maximum distance between predicted and observed cumulative distribution functions. Finally, we repeated the same calculations for the original METE models and for the four other phenomenological models.

2.4 | Metabolic scaling and energy predictions

The FP-METE model estimated b and the Lagrange multipliers by fitting the predicted rescaled ISD (Equation 1) to the observed size data using the maximum likelihood method. By refitting the model predictions to each of the 1000 bootstrap samples, we obtained 1000 maximum likelihood estimates of b for mountain beech. We then used these 1000 estimates to build the corresponding 95% confidence interval (CI) of b (with 2.5% percentile and 97.5% percentile as lower bound and upper bound, respectively). Similarly, we also calculated the 95% CI of the difference of b between post- and pre-earthquake mountain beech (b_{post}-b_{pre}, where b_{pre} and b_{post} denote, respectively, the metabolic scaling exponent pre- and post-earthquake). If the 95% CI of b_{post}-b_{pre} does not include zero, then it means that the exponent has changed significantly.

The scaling exponent b estimated from the FP-METE models allows us to quantify the total energy use within mountain beech. Specifically, we first calculated the total rescaled metabolic rate energy ($E_0 = \Sigma s^b$) within the mountain beech before and after the earthquake. We also calculated the temperature-adjusted total metabolic rate energy using the metabolic rate formula (Ernest et al., 2009): $B = \Sigma size^b e^{-E/kT}$. Here size is the measured (diameter at breast height) or calculated (height and aboveground biomass) individual size from the raw data; E is the activation energy (0.32 eV, Allen et al., 2005); k is the Boltzmann's constant (8.6×10^{-5} eVK^{-1}, Allen et al., 2005); and T is the mean annual temperature in Kelvin pre- (282.08 K) and post-earthquake (281.67 K). We repeated the calculations for the 1000 bootstrap samples to

detect if any trend in the total metabolic rate energy is a sampling artefact. For comparison, we repeated the calculations of E_0 and B using the universal values of b predicted from the MST in the SI.

Our estimate of b from the FP-METE model also allows us to predict the relationship between energy and size across plots, and the change in the relationship pre- and post-earthquake. We calculated E_0 within each plot for the mountain beech before and after the earthquake separately. We fitted simple linear regression and quadratic regression to the log-transformed E_0 against log-transformed mean individual size, and obtained their slope and quadratic coefficient estimates, respectively. We repeated these analyses for each bootstrap sample and obtained the 95% CI of the slope (c) and squared coefficient, using 2.5% and 97.5% percentiles of the corresponding estimate from 1000 bootstrap samples as the lower and upper bounds, respectively. A positive c would indicate that more energy is allocated to plots with larger-sized individuals. A negative c would indicate that more energy is allocated to plots with smaller-sized individuals. If c is not significantly different from zero, then it implies that the energy is evenly distributed across plots with different-sized individuals. The last scenario would mean that the mountain beech population reaches energy equivalence (White, Ernest, et al., 2007). For comparison, we analysed the energy–size relationship using the universal values of b predicted from the MST in the SI. We did not analyse the relationship between B and mean individual size, because temperature adjustment would not have changed the relationship within pre- or post-earthquake population.

All statistical analysis and modelling were performed in R (R Core Team, 2020). For the original METE and the PP-METE models, β (sum of the Lagrange multipliers) was solved using the nonlinear equation solver 'nleqslv' from the *nleqslv* package (Hasselman, 2018). Maximum likelihood estimations were performed using the 'optim' function of the *stats* package (R Core Team, 2020). Quantiles and cumulative distributions functions for all models were obtained using the *pdqr* package (Chasnovski, 2021). R code is provided in the Supporting Information online.

3 | RESULTS

3.1 | Goodness of fit of METE models to observed size distribution

The FP-METE model (Equation 1) predicted the ISD of mountain beech well, except for overestimating the number of small-sized trees for the post-earthquake data (Figure 1). The PP-METE model

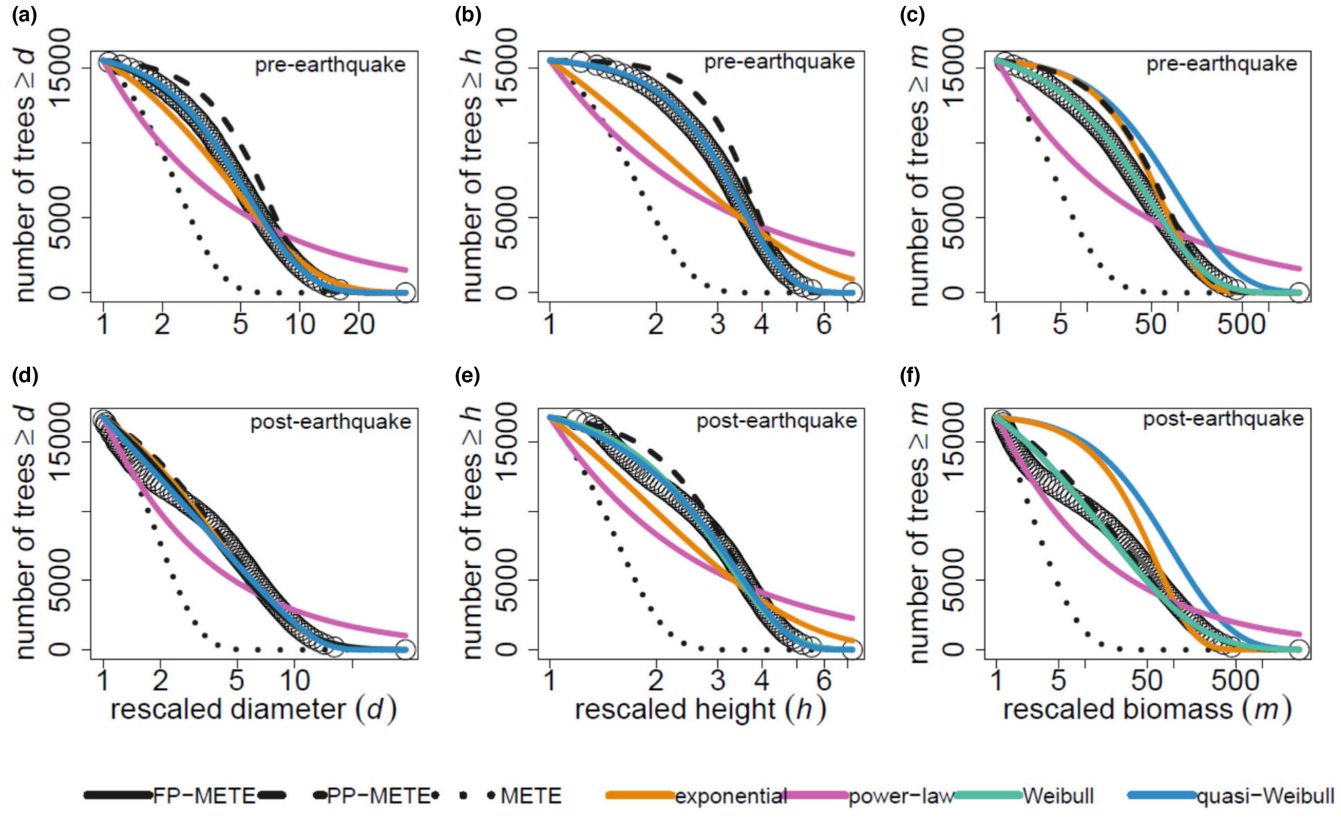

FIGURE 1 Number of individual mountain beech trees above a certain rescaled size against the corresponding rescaled size (d for the rescaled diameter at breast height, h for the rescaled height and m for the rescaled aboveground biomass). The abscissa is on the logarithmic scale, and the ordinate is on the arithmetic scale. For pre- (a–c) and post-earthquake (d–f) mountain beech, observed numbers of trees are denoted by black open circles. To avoid overlap, we plotted only every 200th tree (when ranked by size). The curves show the number of trees predicted by the seven models (see the colour legend at the bottom of the figure). For d and h, the predictions of FP-METE, Weibull and quasi-Weibull overlapped with each other. For m, the predictions of FP-METE and Weibull overlapped with each other. FP-METE, fully parameterized maximum entropy theory of ecology.

overestimated the number of small-sized trees and the original METE model underestimated the number of trees across all sizes. For *m*, pre- and post-earthquake, FP-METE and Weibull had the lowest AICc (Table 2). For the other combinations of data and measures, quasi-Weibull had the lowest AICc, and FP-METE and Weibull had the second lowest AICc. Model comparison using the bootstrap samples showed similar results and was given in the SI (Figures S4.1–S4.12).

R^2 for the FP-METE model (Equation 1) was above 0.97 in all cases (Table 3) and was the highest among all models for *m* (Table S3.1). Pre-earthquake, *p*-values of the K–S test for the FP-METE models were greater than 0.01 for *h* and *m*, but not for *d* (Table 3). Post-earthquake, none of the models (including FP-METE) yielded a *p*-value greater than 0.01 in any case. The *p*-value for the Weibull model and the quasi-Weibull model was greater than 0.01 in, respectively, two and one out of the six cases (2 data×3 measures; Table S3.2). FP-METE models had the lowest test statistics of the one-sample K–S test among all models for pre-earthquake *h* and for post-earthquake *m* (Table S3.3).

3.2 | Changes in metabolic scaling and energy use pre- and post-earthquake

The 95% CI of *b* estimated from the FP-METE model (Equation 1) was less than the corresponding value predicted by MST for all data and measures, except for pre-earthquake *h* (where the interval contained 3; Table 3, Figure 2). Regardless of measures, the 95% CI of the difference in *b* between post- and pre-earthquake data (b_{post}-b_{pre}) was less than zero (Figure 2).

The total rescaled metabolic rate energy, E_0, and temperature-adjusted total metabolic rate energy, *B*, decreased substantially after the earthquake (Table 3, Figure 3). Depending on size measures, post-earthquake E_0 decreased by 66.2%–67.8% compared to pre-earthquake E_0. Similarly, post-earthquake *B* decreased by 66.7%–85.2% compared to pre-earthquake *B*. The analysis using bootstrap samples showed a consistent decline of *B* after the earthquake in all but two samples for all measures (Figure 3).

The slope of the energy-size relationship (*c*) differed significantly from zero for *h*, but not for *d* or *m* before the earthquake (Table 3, Figure 4). The value of *c* was significantly positive for *h*, significantly negative for *m*, and not different from zero for *d* after the earthquake. Point estimates of *c* consistently declined from before to after the earthquake for each measure. The quadratic coefficient of the quadratic regression did not differ significantly from zero for any combination of data and measure. Point estimates of *c* using MST increased from before to after the earthquake for *d* and *m*, decreased for *h* (Table S2.2).

4 | DISCUSSION

4.1 | Goodness of fit of the FP-METE model

Our analyses showed that the FP-METE model reasonably predicted the ISD of mountain beech, under various size measures before and

TABLE 2 AICc values of individual size distribution models, including FP-METE, PP-METE, METE (original METE) and four phenomenological distribution models (see Section 2), for the pre- and post-earthquake mountain beech population under different rescaled size measures (*d*, *h* and *m*, see Table 1). Integers and percentages in the parentheses denote, respectively, the model rankings (in ascending order of AICc) and the AICc weights. If the difference in AICc between two models is less than two, then the two models are of the same rank. Bold indicates the best model according to AICc. FP-METE and Weibull models have the same AICc (to the ones position) due to their similar functional forms (Equation 1, see Methods and Forbes et al., 2011). But the parameters of these two models have different interpretations.

Data	Rescaled size measure	AICc						
		FP-METE	PP-METE	METE	Exponential	Power-law	Weibull	Quasi-Weibull
Pre-earthquake	*d*	76,205 (2, 0.0%)	79,601 (5, 0.0%)	203,522 (7, 0.0%)	77,870 (4, 0.0%)	91,235 (6, 0.0%)	76,205 (2, 0.0%)	**76,123 (1, 100%)**
	h	44,203 (2, 0.0%)	48,634 (4, 0.0%)	169,714 (7, 0.0%)	55,266 (5, 0.0%)	68,214 (6, 0.0%)	44,203 (2, 0.0%)	**44,180 (1, 100%)**
	m	**159,089 (1, 48.6%)**	161,696 (3, 0.0%)	284,942 (7, 0.0%)	162,522 (4, 0.0%)	173,492 (6, 0.0%)	**159,089 (1, 51.4%)**	164,068 (5, 0.0%)
Post-earthquake	*d*	79,744 (2, 0.0%)	80,018 (5, 0.0%)	313,307 (7, 0.0%)	79,799 (4, 0.0%)	86,064 (6, 0.0%)	79,744 (2, 0.0%)	**78,516 (1, 100%)**
	h	49,560 (2, 0.0%)	50,425 (4, 0.0%)	274,470 (7, 0.0%)	55,427 (5, 0.0%)	66,404 (6, 0.0%)	49,560 (2, 0.0%)	**49,324 (1, 100%)**
	m	**160,479 (1, 49.9%)**	160,629 (3, 0.0%)	389,412 (7, 0.0%)	173,010 (5, 0.0%)	166,720 (4, 0.0%)	**160,479 (1, 50.1%)**	173,693 (6, 0.0%)

Abbreviations: AICc, Akaike information criterion corrected; FP-METE, fully parameterized maximum entropy theory of ecology; PP-METE, partially parameterized maximum entropy theory of ecology.

TABLE 3 Parameter estimations of the FP-METE model (Equation 1), for the pre- and post-earthquake mountain beech data under different rescaled size measures (*d*, *h* and *m*). R^2 is the coefficient of determination as defined in Section 2. *p* is the *p*-value from the K–S test. Other notations are defined in Table 1. Point estimates are obtained from the actual data. Values within parentheses show the 95% confidence intervals (2.5% and 97.5% percentiles of the corresponding parameter estimates) obtained from the bootstrap samples (see Section 2).

		Rescaled size		
Data	**Parameter**	***d***	***h***	***m***
Pre-earthquake	*n*	15,512	15,512	15,512
	b	1.494 (1.388, 1.616)	3.210 (2.919, 3.520)	0.662 (0.604, 0.721)
	R^2	0.9981	0.9979	0.9995
	p	<0.0001	0.0894	0.0983
	E_0	226,410	884,118	219,090
	B	2.25	55.25	0.36
	c	−0.168 (−0.486, 0.133)	1.505 (1.028, 1.994)	−0.123 (−0.288, 0.031)
Post-earthquake	*n*	16,789	16,789	16,789
	b	0.914 (0.701, 1.153)	2.460 (2.192, 2.854)	0.408 (0.312, 0.514)
	R^2	0.9747	0.9855	0.9708
	p	<0.0001	<0.0001	<0.0001
	E_0	71,082	298,472	70,612
	B	0.37	8.15	0.12
	c	−0.328 (−0.681, 0.003)	0.616 (0.169, 1.105)	−0.271 (−0.457, −0.085)

Abbreviations: FP-METE, fully parameterized maximum entropy theory of ecology; K–S, Kolmogorov–Smirnov.

after disturbance. For *m*, the FP-METE model was the best among all models studied (Table 2). For *d* and *h*, the FP-METE model performed as well as the Weibull model but was worse than the quasi-Weibull model. The advantage of FP-METE over the Weibull-family models is that the former produces a maximum likelihood estimate of the metabolic scaling exponent *b* for mountain beech, which allows us to infer the energy use and partitioning within the species. We found that *b* decreased from before to after the earthquake, leading to a substantial decrease in total metabolic energy use after the earthquake (Table 3 and Figure 3). The plot-level metabolic energy distribution is shifted favourably towards small-sized individuals after the earthquake (Table 3 and Figure 4).

Despite the overall good performance of the FP-METE among the competing models, its goodness of fit deteriorated slightly after the earthquake. First, the *p*-value of the K–S test was less than 0.0001 after the earthquake, regardless of the size measure (Table 3), indicating that the data are not likely from the FP-METE model distribution (Equation 1). Second, for each size measure, R^2 of the FP-METE model was slightly less post-earthquake than pre-earthquake (Table 3). Visually, the FP-METE model overestimated the number of small-sized and large-sized trees after the earthquake (Figure 1 and Figure S4.13). Interestingly, Coomes et al. (2003) and Hurst et al. (2011) showed that the mortality rate was high for small-sized trees and low for intermediate-to-large-sized trees in New Zealand forests. The discrepancy in the predicted tree counts for the FP-METE model may reflect the failure of the maximum entropy framework to incorporate demographic processes for ISD. In particular, neighbourhood competition can lead to slow growth and high mortality rates of small trees (but not so for large trees; Camac et al., 2018; Hurst et al., 2011).

4.2 | Estimation of metabolic scaling exponent and its variability under disturbance

The adequate fit of the FP-METE model to the data gives us confidence about the empirical plausibility of its estimate of the metabolic scaling exponent *b*. In the New Zealand data, predictions of the original METE (assuming constant *b*) and the power-law distribution (from MST) deviated substantially from the observed size distribution (Figure 1). Except for pre-earthquake *h*, the estimate of *b* from the FP-METE model differed significantly from the constant values predicted from the MST (Table 3, Figure 2). These discrepancies may reflect that MST, in assuming steady state (Allen et al., 2005; Duncanson et al., 2015), is not suitable for studying the metabolic scaling in recently disturbed ecosystems. It also suggests that allowing *b* to vary as a free parameter in the METE framework is a useful way to measure the metabolic pace of life after disturbance.

Empirical research on metabolic scaling traditionally estimates *b* from measured body size and some proxy of metabolic rate using a regression approach. In plant studies, respiration rate is often used as a proxy for the metabolic rate. However, measuring whole-plant respiration rate is costly and can be performed only on a limited number of individuals. Another method to estimate the individual metabolic rate assumes that metabolic rate is proportional to tree

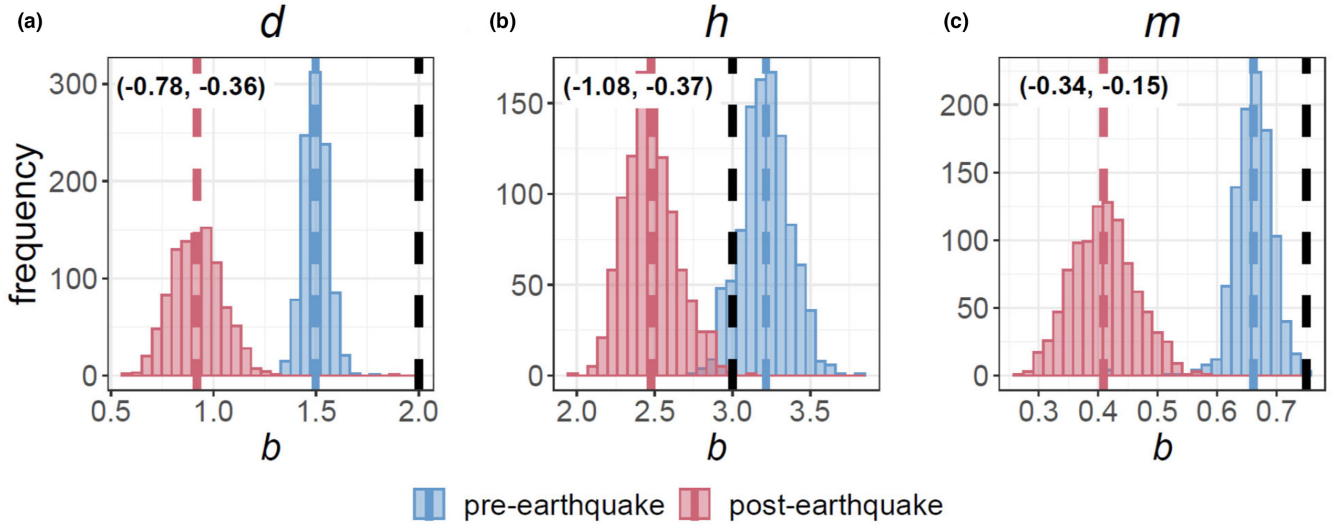

FIGURE 2 Metabolic scaling exponent, *b*, estimated from the FP-METE model (Equation 1) using bootstrap samples of mountain beech, under each rescaled size measure (*d* in (a); *h* in (b) and *m* in (c)). Blue and red bars indicate pre- and post-earthquake estimates, respectively. The blue and red dashed lines show the mean values of *b* from the pre- and post-earthquake samples, respectively. The black dashed lines show the metabolic scaling exponent predicted by the MST (2 for *d*, 3 for *h* and 0.75 for *m*). Values in parentheses show the 95% CI of the difference in *b* between post-earthquake and pre-earthquake (b_{post}-b_{pre}). FP-METE, fully parameterized maximum entropy theory of ecology; MST, metabolic scaling theory.

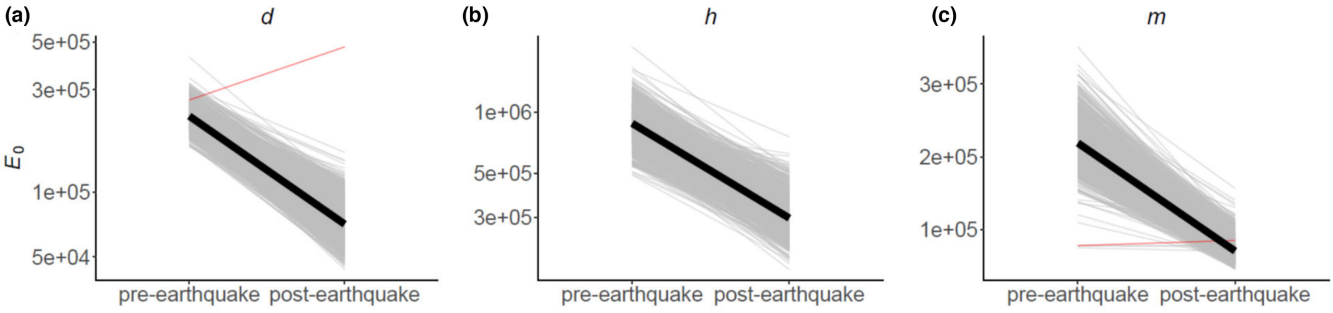

FIGURE 3 Changes in total rescaled metabolic rate energy, E_0, before and after the earthquake using each size measure (*d* in (a); *h* in (b) and *m* in (c)). The grey and red lines show, respectively, whether the energy decreases or increases from pre- to post-earthquake, using the 1000 bootstrap samples. The dark black lines show the change in E_0 using the actual data.

crown volume (Anfodillo et al., 2013; Sellan et al., 2017), but the accuracy of such method depends on the reliability of tree allometry used to predict crown volume. An efficient method to estimate *b* at the community or population level has been lacking. Our FP-METE model, relying on the macro-state constraints of the studied system and treating *b* as a free parameter, obtains the most likely value of population-level *b* from the empirical ISD, without the need for individual metabolic rate measurements. It expands the predictive scope of the original METE and provides a novel method of estimating metabolic scaling beyond the individual level. An important question for future research is how close the estimated *b* from the FP-METE model is to the value obtained from the traditional regression method.

Multiple factors have been found to correlate with the variation of *b* in animal species, such as lifestyle, activity level and temperature (Glazier, 2005). Similar analyses are rare for plant species, due to the difficulty in obtaining the metabolic rate proxy of plant organisms. This has impeded the understanding of the variation of *b* in disturbed ecosystems. In an experimental analysis of the whole plant respiration rate (Mori et al., 2010), it was found that *b* experienced a shift from small plants (≈1) to large plants (≈0.75), reflecting the effect of ontogenetic state on plant metabolic scaling. Our result gives the first evidence of significant decline of *b* within a plant species as the population recovers from a strong earthquake disturbance. Biological understanding of the potential mechanisms of change in *b* still needs further research. Duncanson et al. (2015) argued that forests that do not experience disturbance or environmental change should shift towards the prediction of MST with constant *b*. However, such an argument is difficult to test, as any forest ecosystem is subject to natural disturbance and will be influenced by other, external factors. Using a theoretical model of maximal lifetime reproduction,

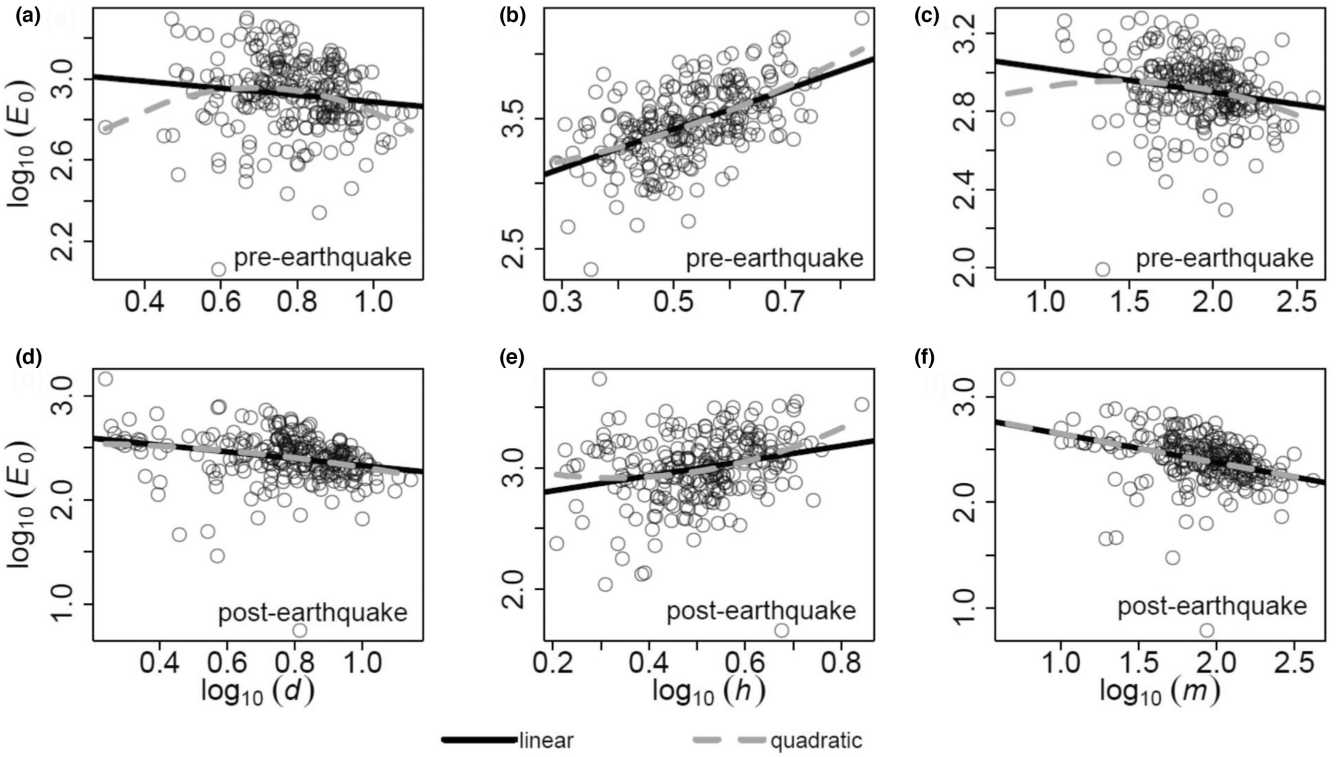

FIGURE 4 Total rescaled metabolic rate energy (E_0) against the mean individual size (d, h or m) on log–log scale, before (a–c) and after earthquake (d–f). Each open circle represents E_0 and the mean individual size from a single plot. Solid black and dashed grey lines show, respectively, the least-squares linear and quadratic regression lines fitted to the log-transformed variables.

White et al. (2022) predicted that increased mortality during the Anthropocene will cause b to decrease. Whether the change in b that we estimated from the New Zealand data can be explained by the demographic variation is an open question. Regardless of the mechanism, the change in b has a profound implication on energy use within the studied ecosystem.

4.3 | Disturbance affects metabolic energy flux and distribution

Past estimates of forest carbon or energy flux used constant b from the MST (Allen et al., 2005; Ernest et al., 2009; Price et al., 2010). For example, Ernest et al. (2009) used the universal metabolic rate scaling with tree diameter to show that the total metabolic rate energy was stable over a 15-year period in a 50-ha permanent plot of the Barro Colorado Island. In non-plant ecosystems, disturbance has been found to interact with temperature to influence energy use. Homyack et al. (2011) showed that temperature increase caused by disturbance leads to a higher energy requirement for basic maintenance costs of salamander species. Schwarz et al. (2017) showed that warming and disturbance together accelerate the change of energy flux in soil food webs, but that the specific interaction effect depends on the trophic group.

In the New Zealand data, using the universal b of the MST revealed a consistent decline in the rescaled metabolic rate energy (E_0) and temperature-adjusted metabolic rate energy (B) (Table S2.1). Depending on size measure, E_0 dropped by 1.0%–7.1% from pre-earthquake to post-earthquake, and B decreased by 2.8%–8.5%. In contrast, our FP-METE model predicted a much more dramatic energy decline after a disturbance event (Table 3). Since MST and original METE did not capture the decrease in b, they consequently led to a severe underestimation of the energy decline after the earthquake. This finding has two implications. First, despite a large cohort of recruitment after a much earlier disturbance event (Allen et al., 2020; Hurst et al., 2011) that increased the number of individuals post-earthquake (1277 more mountain beech trees), an increase in abundance alone is not enough to compensate for the total metabolic energy decline. Second, these declines mean that the change in the ISD alone is not sufficient to capture the impact of disturbance on total forest energy use. Incorporating changes in metabolic scaling as a consequence of the disturbance event is therefore necessary to derive accurate estimates of the total energy changes of the mountain beech populations.

Research on the energy distribution among different-sized individuals (e.g. energy equivalence) suffers from conceptual and methodological problems (Isaac et al., 2013, see Introduction). Previous testing of the relationship between metabolic energy use and body size for disturbed ecosystems is even more rudimentary. In an empirical study of soil invertebrates, Ehnes et al. (2014) showed that population-level energy use increases with body size, with land use types (forest succession stages) having a marginal effect on

the relationship. They found a shallower slope of the energy–size relationship for soil–animal communities in more intensively used forests. In our analysis, before the earthquake, the slope of the energy–size relationship did not differ significantly from zero for diameter and aboveground biomass, which is consistent with the hypothesis of energy equivalence. The slope was significantly positive for height (Table 3, Figure 4), suggesting that mountain beech may allocate more metabolic energy to vertical growth in taller trees to compete for the canopy space related to photosynthesis. Mountain beech is a light-demanding species, and competition for light was relatively intense pre-earthquake (Hurst et al., 2011). After the earthquake, the slope of the energy–size relationship decreased regardless of size measure, resulting in a marginally negative slope for diameter and a significantly negative slope for aboveground biomass. This means that more metabolic energy is distributed towards smaller trees measured by diameter and aboveground biomass. On the other hand, the slope was still significantly positive for height, although with a smaller magnitude, suggesting a diminished energetic advantage for taller trees. These observations can be attributed to the smaller *b* after disturbance, which had a stronger negative effect on the energy use for larger-sized individuals. The change in size distribution alone (without considering the variation in metabolic scaling) did not reveal a consistent change in energy distribution after disturbance (Table S2.2).

We found that the 'energy-equivalence' hypothesis is not universally true, but depends on the size measure and disturbance history of the mountain beech population in the New Zealand forest (Table 3). First, the biology of the studied species can dictate the direction of energy allocation to individuals of varying sizes. Second, after disturbance, metabolic energy is predominately allocated to small-sized individuals at the population level, thus breaking the observed energy equivalence for the pre-earthquake mountain beech with respect to diameter and aboveground biomass. We speculate that in this ecosystem, metabolic energy redistribution may be a response to the forest gaps caused by landslides during the earthquake or the regeneration pulse from pre-1980 disturbance (Allen et al., 2020). Future test of the energy equivalence must consider the effects of species biology, size distribution and metabolic scaling. It remains unclear whether *b* will decrease in other (plant and non-plant) populations undergoing disturbance. However, our approach to quantifying the metabolic energy repartitioning after disturbance should be broadly applicable across taxa, disturbance types and spatial scales.

4.4 | Summary and conclusions

To better understand the usefulness of the FP-METE for modelling macroecological patterns in disturbed ecosystems, it is necessary to conduct similar tests for other distributions and scaling relationships using data at various taxonomic, temporal and spatial scales. For example, predictions of our FP-METE models rely on the power-law scaling form between individual metabolic rate and individual body size. To understand the effect of such a form on model predictions, comparable studies that involve various metabolic scaling relationships and models (e.g. Muller-Landau et al., 2006) are useful. Furthermore, our analysis treated all plots in the forest as a single population and did not reveal the earthquake effects at the plot level. For example, various characteristics of each plot (e.g. topography and distance to the epicentre of the earthquake) can influence tree recruitment and death within that plot (Allen et al., 2020). Spatially explicit models may be needed to investigate plot-level responses to disturbance.

Recent works have coupled METE with other mechanistic models, for example, with the unified neutral theory of biodiversity (Hubbell, 2001; O'Dwyer et al., 2017), and with dynamic mechanisms (Harte et al., 2021), in an attempt to improve the predictive power of METE models, especially for ecosystems under disturbance. Compared with these coupled models, which require specific probability distributions or detailed dynamics of the ecosystem, our parameterized METE models do not rely on external mechanisms and instead obtain the optimal solutions (i.e. maximum entropy) with information and constraints based solely on empirical data. In essence, the parameterized METE models predict patterns at a snapshot of the succession history of an ecosystem and, therefore, are appropriate to compare changes before and after disturbance (i.e. pre- and post-earthquake in this work).

It has been suggested that the poor performance of the original METE model in predicting macroecological patterns is because the Shannon entropy quantifies an ecosystem in a state of demographic equilibrium (Newman et al., 2020). Results from our FP-METE models indicate that the static METE framework is capable of modelling ecosystems under disturbance when the metabolic scaling exponent and Lagrange multipliers are treated as population-specific parameters. Our results suggest that FP-METE models are a promising candidate for modelling the ISD in disturbed ecosystems and the estimation of metabolic scaling exponent using an informatics approach. In turn, these results could be extended to predictions of timelines for forest recovery, vulnerability of aboveground carbon stocks, and other structural and ecological patterns that affect ecosystem functioning and services.

AUTHOR CONTRIBUTIONS

MX conceived the idea and performed the analysis. MX and RA designed the study. All authors wrote the first draft of the paper and contributed substantially to subsequent versions of the manuscript.

ACKNOWLEDGEMENTS

We thank John Wardle for establishing the New Zealand tree plot network used in this study, and Kevin Platt, Larry Burrows, Susan Wiser and many others who collected, checked and archived the data. Work on these data were funded by the former New Zealand Forest Service, Manaaki Whenua-Landcare Research and the

authors. The study area falls within the rohe of Ngāi Tahu. We thank John Harte, Micah Brush, Kaito Umemura and two anonymous reviewers for comments on an earlier version of the manuscript. We did not receive any financial support for this work.

CONFLICT OF INTEREST STATEMENT

The authors declare that they have no conflict of interest.

DATA AVAILABILITY STATEMENT

The raw data and the R code used to perform the analysis in this work are available in the Supporting Information.

ORCID

Meng Xu https://orcid.org/0000-0002-2569-3654

REFERENCES

Alberti, M. (2005). The effects of urban patterns on ecosystem function. *International Regional Science Review*, *28*, 168–192.

Allen, A. P., Gillooly, J. F., & Brown, J. H. (2005). Linking the global carbon cycle to individual metabolism. *Functional Ecology*, *19*, 202–213.

Allen, R. B., Bellingham, P. J., & Wiser, S. K. (1999). Immediate damage by an earthquake to a temperate montane forest. *Ecology*, *80*, 708–714.

Allen, R. B., MacKenzie, D. I., Bellingham, P. J., Wiser, S. K., Arnst, E. A., Coomes, D. A., & Hurst, J. M. (2020). Tree survival and growth responses in the aftermath of a strong earthquake. *Journal of Ecology*, *108*, 107–121.

Anfodillo, T., Carrer, M., Simini, F., Popa, I., Banavar, J. R., & Maritan, A. (2013). An allometry-based approach for understanding forest structure, predicting tree-size distribution and assessing the degree of disturbance. *Proceedings of the Royal Society B*, *280*, 20122375.

Arnadottir, T., Beavan, J., & Pearson, C. (1995). Deformation associated with the 18 June 1994 Arthur's pass earthquake, New Zealand. *New Zealand Journal of Geology and Geophysics*, *38*, 553–558.

Attiwill, P. M. (1994). The disturbance of forest ecosystems: The ecological basis for conservative management. *Forest Ecology and Management*, *63*, 247–300.

Bailey, R. L., & Dell, T. R. (1973). Quantifying diameter distributions with the Weibull function. *Forest Science*, *19*, 97–104.

Barlow, J., Lennox, G. D., Ferreira, J., Berenguer, E., Lees, A. C., Mac Nally, R., Thomson, J. R., de Barros Ferraz, S. F., Louzada, J., Oliveira, V. H. F., Parry, L., de Castro Solar, R. R., Vieira, I. C. G., Aragão, L. E. O. C., Begotti, R. A., Braga, R. F., Cardoso, T. M., de Oliveira, R. C., Jr., Souza, C. M., Jr., … Gardner, T. A. (2016). Anthropogenic disturbance in tropical forests can double biodiversity loss from deforestation. *Nature*, *535*, 144–147.

Barnes, A. D., Jochum, M., Lefcheck, J. S., Eisenhauer, N., Scherber, C., O'Connor, M. I., de Ruiter, P., & Brose, U. (2018). Energy flux: The link between multitrophic biodiversity and ecosystem functioning. *Trends in Ecology & Evolution*, *33*, 186–197.

Bertsekas, D. P. (2014). *Constrained optimization and Lagrange multiplier methods*. Academic Press.

Bokma, F. (2004). Evidence against universal metabolic allometry. *Functional Ecology*, *18*, 184–187.

Brawn, J. D., Robinson, S. K., & Thompson, F. R., III. (2001). The role of disturbance in the ecology and conservation of birds. *Annual Review of Ecology and Systematics*, *32*, 251–276.

Brummer, A. B., & Newman, E. A. (2019). Derivations of the core functions of the maximum entropy theory of ecology. *Entropy*, *21*, 712.

Brush, M. J., Matthews, T., Borges, P. A. V., & Harte, J. (2022). Land use change through the lens of macroecology: Insights from Azorean arthropods and the maximum entropy theory of ecology. *Ecography*, *8*, e06141.

Camac, J. S., Condit, R., FitzJohn, R. G., McCalman, L., Steinberg, D., Westoby, M., Wright, S. J., & Falster, D. S. (2018). Partitioning mortality into growth-dependent and growth-independent hazards across 203 tropical tree species. *Proceedings of the National Academy of Sciences of the United States of America*, *115*, 12459–12464.

Cardinale, B. J., & Palmer, M. A. (2002). Disturbance moderates biodiversity–ecosystem function relationships: Experimental evidence from caddisflies in stream mesocosms. *Ecology*, *83*, 1915–1927.

Chasnovski, E. (2021). pdqr: Work with custom distribution functions. R package version 0.3.0. https://CRAN.R-project.org/package=pdqr

Coomes, D. A., Duncan, R. P., Allen, R. B., & Truscott, J. (2003). Disturbances prevent stem size-density distributions in natural forests from following scaling relationships. *Ecology Letters*, *6*, 980–989.

Coomes, D. A., Holdaway, R. J., Kobe, R. K., Lines, E. R., & Allen, R. B. (2012). A general integrative framework for modelling woody biomass production and carbon sequestration rates in forests. *Journal of Ecology*, *100*, 42–64.

Cottingham, K. L., & Zens, M. S. (2004). Metabolic rate opens a grand vista on ecology. *Ecology*, *85*, 1805–1807.

Courtois, R., Ouellet, J. P., Breton, L., Gingras, A., & Dussault, C. (2007). Effects of forest disturbance on density, space use, and mortality of woodland caribou. *Ecoscience*, *14*, 491–498.

Cuddington, K. (2011). Legacy effects: The persistent impact of ecological interactions. *Biological Theory*, *6*, 203–210.

Damuth, J. (1981). Population density and body size in mammals. *Nature*, *290*, 699–700.

Danneyrolles, V., Dupuis, S., Fortin, G., Leroyer, M., de Römer, A., Terrail, R., Vellend, M., Boucher, Y., Laflamme, J., Bergeron, Y., & Arseneault, D. (2019). Stronger influence of anthropogenic disturbance than climate change on century-scale compositional changes in northern forests. *Nature Communications*, *10*, 1265.

DeAngelis, D. L., Waterhouse, J. C., Post, W. M., & O'Neill, R. V. (1985). Ecological modelling and disturbance evaluation. *Ecological Modelling*, *29*, 399–419.

Deng, J. M., Li, T., Wang, G. X., Liu, J., Yu, Z. L., Zhao, C. M., Ji, M. F., Zhang, Q., & Liu, J. Q. (2008). Trade-offs between the metabolic rate and population density of plants. *PLoS ONE*, *3*(3), e1799.

Dornelas, M. (2010). Disturbance and change in biodiversity. *Philosophical Transactions of the Royal Society B*, *365*, 3719–3727.

Duncanson, L. I., Dubayah, R. O., & Enquist, B. J. (2015). Assessing the general patterns of forest structure: Quantifying tree and forest allometric scaling relationships in the United States. *Global Ecology and Biogeography*, *24*, 1465–1475.

Ehnes, R. B., Pollierer, M. M., Erdmann, G., Klarner, B., Eitzinger, B., Digel, C., Ott, D., Maraun, M., Scheu, S., & Brose, U. (2014). Lack of energetic equivalence in forest soil invertebrates. *Ecology*, *95*, 527–537.

Enquist, B. J., & Niklas, K. J. (2001). Invariant scaling relations across tree-dominated communities. *Nature*, *410*, 655–660.

Ernest, S. M., White, E. P., & Brown, J. H. (2009). Changes in a tropical forest support metabolic zero-sum dynamics. *Ecology Letters*, *12*, 507–515.

Fitzhugh, R. D., Driscoll, C. T., Groffman, P. M., Tierney, G. L., Fahey, T. J., & Hardy, J. P. (2001). Effects of soil freezing disturbance on soil solution nitrogen, phosphorus, and carbon chemistry in a northern hardwood ecosystem. *Biogeochemistry*, *56*, 215–238.

Forbes, C., Evans, M., Hastings, N., & Peacock, B. (2011). *Statistical distributions* (4th ed.). Wiley.

Franzman, J., Brush, M., Umemura, K., Ray, C., Blonder, B., & Harte, J. (2021). Shifting macroecological patterns and static theory failure in a stressed alpine plant community. *Ecosphere*, *12*, e03548.

Ghedini, G., Malerba, M. E., & Marshall, D. J. (2020). How to estimate community energy flux? A comparison of approaches reveals that size-abundance trade-offs alter the scaling of community energy flux. *Proceedings of the Royal Society B*, *287*, 20200995.

Glazier, D. S. (2005). Beyond the '3/4-power law': Variation in the intra- and interspecific scaling of metabolic rate in animals. *Biological Reviews*, *80*, 611–662.

Glazier, D. S. (2022). Variable metabolic scaling breaks the law: From 'Newtonian' to 'Darwinian' approaches. *Proceedings of the Royal Society B*, *289*, 20221605.

Hamilton, C. (2015). Getting the Anthropocene so wrong. *The Anthropocene Review*, *2*, 102–107.

Harcombe, P. A., Allen, R. B., Wardle, J. A., & Platt, K. H. (1997). Spatial and temporal patterns in stand structure, biomass, growth, and mortality in a monospecific *Nothofagus solandri* var. *cliffortioides* (Hook, f.) Poole forest in New Zealand. *Journal of Sustainable Forestry*, *6*, 313–345.

Harte, J. (2011). *Maximum entropy and ecology: A theory of abundance, distribution, and energetics*. Oxford University Press.

Harte, J., Brush, M., Newman, E. A., & Umemura, K. (2022). An equation of state unifies diversity, productivity, abundance and biomass. *Communications Biology*, *5*, 874.

Harte, J., & Kitzes, J. (2015). Inferring regional-scale species diversity from small-plot censuses. *PLoS ONE*, *10*, e0117527.

Harte, J., & Newman, E. A. (2014). Maximum information entropy: A foundation for ecological theory. *Trends in Ecology & Evolution*, *29*, 384–389.

Harte, J., Newman, E. A., & Rominger, A. J. (2017). Metabolic partitioning across individuals in ecological communities. *Global Ecology and Biogeography*, *26*, 993–997.

Harte, J., Smith, A. B., & Storch, D. (2009). Biodiversity scales from plots to biomes with a universal species–area curve. *Ecology Letters*, *12*, 789–797.

Harte, J., Umemura, K., & Brush, M. (2021). DynaMETE: A hybrid MaxEnt-plus-mechanism theory of dynamic macroecology. *Ecology Letters*, *24*, 935–949.

Harte, J., Zillio, T., Conlisk, E., & Smith, A. B. (2008). Maximum entropy and the state-variable approach to macroecology. *Ecology*, *89*, 2700–2711.

Hasselman, B. (2018). Nleqslv: Solve systems of nonlinear equations. R package version 3.3.2. https://CRAN.R-project.org/package=nleqslv.

Hayward, A., Khalid, M., & Kolasa, J. (2009). Population energy use scales positively with body size in natural aquatic microcosms. *Global Ecology and Biogeography*, *18*, 553–562.

Helmus, M. R., Keller, W., Paterson, M. J., Yan, N. D., Cannon, C. H., & Rusak, J. A. (2010). Communities contain closely related species during ecosystem disturbance. *Ecology Letters*, *13*, 162–174.

Homyack, J. A., Haas, C. A., & Hopkins, W. A. (2011). Energetics of surface-active terrestrial salamanders in experimentally harvested forest. *The Journal of Wildlife Management*, *75*, 1267–1278.

Hubbell, S. P. (2001). *The unified neutral theory of biodiversity and biogeography (MPB-32)*. Princeton University Press.

Hubbell, S. P., Foster, R. B., O'Brien, S. T., Harms, K. E., Condit, R., Wechsler, B., Wright, S. J., & De Lao, S. L. (1999). Light-gap disturbances, recruitment limitation, and tree diversity in a neotropical forest. *Science*, *283*, 554–557.

Hurst, J. M., Allen, R. B., Coomes, D. A., & Duncan, R. P. (2011). Size-specific tree mortality varies with neighbourhood crowding and disturbance in a montane Nothofagus forest. *PLoS ONE*, *6*, e26670.

Isaac, N. J., Storch, D., & Carbone, C. (2013). The paradox of energy equivalence. *Global Ecology and Biogeography*, *22*, 1–5.

Jaynes, E. T. (1957). Information theory and statistical mechanics. *Physical Review*, *106*, 620–630.

Jaynes, E. T. (2003). *Probability theory: The logic of science*. Cambridge University Press.

Jenkins, D. G. (2011). Ranked species occupancy curves reveal common patterns among diverse metacommunities. *Global Ecology and Biogeography*, *20*, 486–497.

Johnstone, J. F., Allen, C. D., Franklin, J. F., Frelich, L. E., Harvey, B. J., Higuera, P. E., Mack, M. C., Meentemeyer, R. K., Metz, M. R., Perry, G. L. W., Schoennagel, T., & Turner, M. G. (2016). Changing disturbance regimes, ecological memory, and forest resilience. *Frontiers in Ecology and the Environment*, *14*, 369–378.

Kleiber, M. (1947). Body size and metabolic rate. *Physiological Reviews*, *27*, 511–541.

Kleinman, J. S., Goode, J. D., Fries, A. C., & Hart, J. L. (2019). Ecological consequences of compound disturbances in forest ecosystems: A systematic review. *Ecosphere*, *10*, e02962.

Kohyama, T., Suzuki, E., Partomihardjo, T., Yamada, T., & Kubo, T. (2003). Tree species differentiation in growth, recruitment and allometry in relation to maximum height in a Bornean mixed dipterocarp forest. *Journal of Ecology*, *91*, 797–806.

Lai, J., Coomes, D. A., Du, X., Hsieh, C. F., Sun, I. F., Chao, W. C., Mi, X., Ren, H., Wang, X., Hao, Z., & Ma, K. (2013). A general combined model to describe tree-diameter distributions within subtropical and temperate forest communities. *Oikos*, *122*, 1636–1642.

McGill, B. J. (2010). Towards a unification of unified theories of biodiversity. *Ecology Letters*, *13*, 627–642.

McGlinn, D. J., Xiao, X., Kitzes, J., & White, E. P. (2015). Exploring the spatially explicit predictions of the maximum entropy theory of ecology. *Global Ecology and Biogeography*, *24*, 675–684.

McGlinn, D. J., Xiao, X., & White, E. P. (2013). An empirical evaluation of four variants of a universal species–area relationship. *PeerJ*, *1*, e212.

Medel, R. G., Bozinovic, F., & Novoa, F. F. (1995). The mass exponent in population energy use: The fallacy of averages reconsidered. *The American Naturalist*, *145*, 155–162.

Mori, S., Yamaji, K., Ishida, A., Prokushkin, S. G., Masyagina, O. V., Hagihara, A., Hoque, A. T. M. R., Suwa, R., Osawa, A., Nishizono, T., Ueda, T., Kinjo, M., Miyagi, T., Kajimoto, T., Koike, T., Matsuura, Y., Toma, T., Zyryanova, O. A., Abaimov, A. P., … Umari, M. (2010). Mixed-power scaling of whole-plant respiration from seedlings to giant trees. *Proceedings of the National Academy of Sciences of the United States of America*, *107*, 1447–1451.

Moser, J. W., Jr. (1972). Dynamics of an uneven-aged forest stand. *Forest Science*, *18*, 184–191.

Muller-Landau, H. C., Condit, R. S., Harms, K. E., Marks, C. O., Thomas, S. C., Bunyavejchewin, S., Chuyong, G., Co, L., Davies, S., Foster, R., Gunatilleke, S., Gunatilleke, N., Hart, T., Hubbell, S. P., Itoh, A., Kassim, A. R., Kenfack, D., LaFrankie, J. V., Lagunzad, D., … Gunatilleke, S. (2006). Comparing tropical forest tree size distributions with the predictions of metabolic ecology and equilibrium models. *Ecology Letters*, *9*, 589–602.

Newman, E. A. (2019). Disturbance ecology in the Anthropocene. *Frontiers in Ecology and Evolution*, *7*, 147.

Newman, E. A., Harte, M. E., Lowell, N., Wilber, M., & Harte, J. (2014). Empirical tests of within-and across-species energetics in a diverse plant community. *Ecology*, *95*, 2815–2825.

Newman, E. A., Wilber, M. Q., Kopper, K. E., Moritz, M. A., Falk, D. A., McKenzie, D., & Harte, J. (2020). Disturbance macroecology: A comparative study of community structure metrics in a high-severity disturbance regime. *Ecosphere*, *11*, e03022.

O'Dwyer, J. P., Rominger, A., & Xiao, X. (2017). Reinterpreting maximum entropy in ecology: A null hypothesis constrained by ecological mechanism. *Ecology Letters*, *20*, 832–841.

Price, C. A., Gilooly, J. F., Allen, A. P., Weitz, J. S., & Niklas, K. J. (2010). The metabolic theory of ecology: Prospects and challenges for plant biology. *New Phytologist*, *188*, 696–710.

R Core Team. (2020). *R: A language and environment for statistical computing*. R Foundation for Statistical Computing, https://www.R-project.org/

Resh, V. H., Brown, A. V., Covich, A. P., Gurtz, M. E., Li, H. W., Minshall, G. W., Reice, S. R., Sheldon, A. L., Wallace, J. B., & Wissmar, R. C. (1988). The role of disturbance in stream ecology. *Journal of the North American Benthological Society*, *7*, 433–455.

Russo, S. E., Robinson, S. K., & Terborgh, J. (2003). Size-abundance relationships in an Amazonian bird community: Implications for the energetic equivalence rule. *The American Naturalist*, *161*, 267–283.

Rybicki, J., & Hanski, I. (2013). Species–area relationships and extinctions caused by habitat loss and fragmentation. *Ecology Letters*, *16*, 27–38.

Santini, L., González-Suárez, M., Rondinini, C., & Di Marco, M. (2017). Shifting baseline in macroecology? Unravelling the influence of human impact on mammalian body mass. *Diversity and Distributions*, *23*, 640–649.

Schwarz, B., Barnes, A. D., Thakur, M. P., Brose, U., Ciobanu, M., Reich, P. B., Rich, R. L., Rosenbaum, B., Stefanski, A., & Eisenhauer, N. (2017). Warming alters energetic structure and function but not resilience of soil food webs. *Nature Climate Change*, *7*, 895–900.

Seidl, R., Rammer, W., & Spies, T. A. (2014). Disturbance legacies increase the resilience of forest ecosystem structure, composition, and functioning. *Ecological Applications*, *24*, 2063–2077.

Sellan, G., Simini, F., Maritan, A., Banavar, J. R., de Haulleville, T., Bauters, M., Doucet, J.-L., Beeckman, H., & Anfodillo, T. (2017). Testing a general approach to assess the degree of disturbance in tropical forests. *Journal of Vegetation Science*, *28*, 659–668.

Sewall, B. J., Freestone, A. L., Hawes, J. E., & Andriamanarina, E. (2013). Size-energy relationships in ecological communities. *PLoS One*, *8*, e68657.

Shannon, C. E. (1948). A mathematical theory of communication. *The Bell System Technical Journal*, *27*, 379–423.

Steffen, W., Crutzen, P. J., & McNeill, J. R. (2007). The Anthropocene: Are humans now overwhelming the great forces of nature. *Ambio*, *36*, 614–621.

Stillman, R. A., West, A. D., Caldow, R. W., & Durell, S. E. L. V. D. (2007). Predicting the effect of disturbance on coastal birds. *Ibis*, *149*, 73–81.

Supp, S. R., & Ernest, S. M. (2014). Species-level and community-level responses to disturbance: A cross-community analysis. *Ecology*, *95*, 1717–1723.

Tait, L. W., & Schiel, D. R. (2011). Legacy effects of canopy disturbance on ecosystem functioning in macroalgal assemblages. *PLoS ONE*, *6*, e26986.

Thom, D., & Seidl, R. (2016). Natural disturbance impacts on ecosystem services and biodiversity in temperate and boreal forests. *Biological Reviews*, *91*, 760–781.

Turner, M. G. (2010). Disturbance and landscape dynamics in a changing world. *Ecology*, *91*, 2833–2849.

Villnäs, A., Norkko, J., Hietanen, S., Josefson, A. B., Lukkari, K., & Norkko, A. (2013). The role of recurrent disturbances for ecosystem multifunctionality. *Ecology*, *94*, 2275–2287.

West, G. B., Brown, J. H., & Enquist, B. J. (1997). A general model for the origin of allometric scaling laws in biology. *Science*, *276*, 122–126.

West, G. B., Brown, J. H., & Enquist, B. J. (1999). A general model for the structure and allometry of plant vascular systems. *Nature*, *400*, 664–667.

White, C. R., Alton, L. A., Bywater, C. L., Lombardi, E. J., & Marshall, D. J. (2022). Metabolic scaling is the product of life-history optimization. *Science*, *377*, 834–839.

White, C. R., Cassey, P., & Blackburn, T. M. (2007). Allometric exponents do not support a universal metabolic allometry. *Ecology*, *88*, 315–323.

White, E. P., Ernest, S. M., Kerkhoff, A. J., & Enquist, B. J. (2007). Relationships between body size and abundance in ecology. *Trends in Ecology & Evolution*, *22*, 323–330.

White, E. P., Thibault, K. M., & Xiao, X. (2012). Characterizing species abundance distributions across taxa and ecosystems using a simple maximum entropy model. *Ecology*, *93*, 1772–1778.

Wilber, M. Q., Kitzes, J., & Harte, J. (2015). Scale collapse and the emergence of the power law species–area relationship. *Global Ecology and Biogeography*, *24*, 883–895.

Wilson, S. D., & Tilman, D. (1991). Interactive effects of fertilization and disturbance on community structure and resource availability in an old-field plant community. *Oecologia*, *88*, 61–71.

Wilson, S. D., & Tilman, D. (1993). Plant competition and resource availability in response to disturbance and fertilization. *Ecology*, *74*, 599–611.

Winfree, R., Griswold, T., & Kremen, C. (2007). Effect of human disturbance on bee communities in a forested ecosystem. *Conservation Biology*, *21*, 213–223.

Wright, A. J., Ebeling, A., De Kroon, H., Roscher, C., Weigelt, A., Buchmann, N., Fischer, C., Hacker, N., Hildebrandt, A., Leimer, S., Mommer, L., Oelmann, Y., Scheu, S., Steinauer, K., Strecker, T., Weisser, W., Wilcke, W., & Eisenhauer, N. (2015). Flooding disturbances increase resource availability and productivity but reduce stability in diverse plant communities. *Nature Communications*, *6*, 1–6.

Xiao, X., McGlinn, D. J., & White, E. P. (2015). A strong test of the maximum entropy theory of ecology. *The American Naturalist*, *185*, E70–E80.

Xu, M. (2020). Parameterized maximum entropy models predict variability of metabolic scaling across tree communities and populations. *Ecology*, *101*, e03011.

Xu, M., Jiang, M., & Wang, H. F. (2021). Integrating metabolic scaling variation into the maximum entropy theory of ecology explains Taylor's law for individual metabolic rate in tropical forests. *Ecological Modelling*, *455*, 109655.

Yamamoto, S. I. (2000). Forest gap dynamics and tree regeneration. *Journal of Forest Research*, *5*, 223–229.

Zeng, C., Xie, Q., Wang, T., Zhang, C., Dong, X., Guan, L., Li, K., & Duan, W. (2017). Stochastic ecological kinetics of regime shifts in a time-delayed lake eutrophication ecosystem. *Ecosphere*, *8*, e01805.

BIOSKETCHES

Meng Xu is an associate professor in the Department of Mathematics at Pace University, New York City. He is broadly interested in ecological scaling and mathematical modelling. His current research focuses on developing ecological models parameterized by scaling relationships.

Robert Allen is an independent researcher in New Zealand. He studies decadal-level forest dynamics in relation to natural and human-induced disturbances. A current emphasis is on using time-series data to determine variability in compositional, structural and functional responses in montane forests.

Erica Newman is a research scientist at the University of Texas at Austin. Her current work integrates methods of macroecology and disturbance ecology for the purpose of understanding biodiversity patterns across scales.

SUPPORTING INFORMATION

Additional supporting information can be found online in the Supporting Information section at the end of this article.

How to cite this article: Xu, M., Allen, R. B., & Newman, E. A. (2023). Earthquake disturbance shifts metabolic energy use and partitioning in a monodominant forest. *Global Ecology and Biogeography*, *00*, 1–16. https://doi.org/10.1111/geb.13711